percent of the tagged *S. patens* from the preceding fall survived, and in Georgia, 27 percent survived. The remaining four species had no over-winter survival of individual culms. The morphology of the surviving culms differed from most stems tagged in May 1975. These culms represented a new age class having unique production and senescence rates.

The data represent one age class of individual culms from the whole plant community. Recruitment during the growing season was evident by the measurement of stem densities (*2*) from quadrat counts performed concurrent with the monitoring of tagged plants. Elongation, leaf production, senescence, and abscission-pattern similarity for the younger culms must be determined before the entire population can be characterized. For plant species that die completely over winter, the initial group of tillers is the most important with respect to ultimate productivity. *Spartina patens* from Delaware and Georgia represent a different situation in which approximately 25 percent of the population survives to the succeeding growing season. The problem of assessing annual primary productivity is complicated by this carry-over of material. The importance of studying individual culms is essential to an understanding of the spatial and temporal variation in overall community production.

Estimates of leaf-abscission and stem-mortality time and numbers indicate some independence of primary productivity from peak standing-crop biomass. The importance of plant biomass additions before peak standing-crop biomass has been suggested (*5*). Attempts to quantify the primary production using the midseason addition would require biomass measurements of each dead leaf and each dead culm of various heights. Calculation of rates of turnover from live to dead standing crops would enhance and validate traditional harvest methods. Geratologic studies of plant tissue within a plant community varies spatially and temporally, demonstrating the need for specific rate measurements for each community.

The continual addition of plant tissue to the marsh system by individual culms indicates the independence of peak standing crop biomass from annual primary production. The effect was more pronounced in the southern latitudes where seasonal climatic changes are less abrupt in controlling plant growth and senescence. The carry-over of plant tissue from the previous year and the production of leaves after cessation of culm elongation in *S. patens* further substantiated the continuum of plant tissue losses.

The dependence of leaf production on culm elongation was evident for *S. alterniflora*, *P. communis*, and *S. cynosuroides*. The similarity of the seasonal pattern of leaf senescence in Delaware and Georgia suggests climatic control of this process. High spring senescence rates were not met with immediately increased abscission rate; rather, a time lag of varying duration existed. Plants with a culm longevity of 1 year had increased mortality rates near winter, and plants with a culm longevity exceeding 1 year had constant seasonal mortality rates.

Each of the growth processes dictates the time and quantity of tissue transition from live to dead and the addition of detritus to the estuarine food web. Residence time of leaves, continual culm mortality, and pulses of detritus export are species dependent and constitute the essential processes controlling primary production that ultimately dictates the value of each plant species to the ecosystem.

MICHAEL A. HARDISKY
ROBERT J. REIMOLD
University of Georgia, Marine Extension Service, Brunswick 31520

References and Notes

1. R. Reimold, J. Gallagher, R. Linthurst, W. Pfeiffer, in *Estuarine Research*, E. Cronin, Ed. (Academic Press, New York, 1975), p. 217; J. Gallagher, R. Reimold, R. Linthurst, W. Pfeiffer, *Ecology*, in press.
2. R. Reimold and R. Linthurst, *The Primary Productivity of Minor Marsh Plants in Delaware, Georgia, and Maine* (Rep. No. DACW 39-73-C-0110, U.S. Army Corps of Engineers, Vicksburg, Miss., 1977), p. 1.
3. R. Reimold and M. Hardisky, in preparation.
4. P. Williamson, *J. Ecol.* **64**, 1059 (1976); I. Bradbury and G. Hofstra, *Ecology* **57**, 209 (1976).
5. C. Kirby and J. Gosselink, *Ecology* **57**, 1052 (1976).
6. Supported by the Office of Dredged Materials Research, U.S. Army Engineer Waterways Experiment Station, Corps of Engineers, Vicksburg, Miss., under contract DACW 39-73-C-0110. We especially thank Dr. J. L. Gallagher and R. A. Linthurst for their contribution to the tagging study. We also thank W. B. Kinter, K. S. Price, and H. Church for logistic support.

25 April 1977; revised 22 June 1977

The Charnockite Geotherm

Abstract. *Charnockite, a hypersthene-bearing granite, and other associated rocks of the charnockite series have a global distribution. These rocks, according to evidence from mineral-chemical and experimental phase equilibrium relations, formed or recrystallized at temperatures between 800° and 900°C and at relatively shallow depths of 6 to 12 kilometers. This evidence indicates the existence of geothermal gradients of 70° to 100°C per kilometer probably at various times, the latest being around 1300 × 10^6 years ago.*

Charnockites are granites containing hypersthene $(Mg,Fe)SiO_3$. Generally they occur in association with rocks or other bulk compositions, and the name "charnockite series" is used for the group of rocks that is related in time and space. In this report I demonstrate that rocks of the charnockite series have formed in chemical equilibrium and provide information on the pressure and temperature of formation. The results may have an important bearing on models of the thermal evolution of the earth.

Charnockites occur in many parts of the world (*1*); they are generally closely associated with metamorphic rocks of the granulite facies and anorthosites. Figure 1 shows the distribution of charnockites and of the rocks of the granulite facies (*2*). However, on the basis of this map, it should not be inferred that charnockites are related in space since they are much older than the time when the breakup of the Pangaea began [200 × 10^6 years before the present (B.P.)] and the configuration of the continents at that time is unknown.

Petrologists generally agree that charnockites are metamorphic rocks which could be of either sedimentary or igneous origin (*3–5*). Hubbard (*5*), for example, has described the in situ charnockitization (*6*) of sedimentary rocks in the Varberg area of Sweden. On the basis of extensive fieldwork, he has distinguished these rocks from a separate charnockite-granite association that is clearly of igneous origin (*7*). Similar field relationships in the occurrences of charnockites have been described from many parts of the world.

The chemical composition of coexisting phases in a rock can be used both to demonstrate the approach of a system to chemical equilibrium during recrystallization (*8*) and to estimate the pressure and temperature of crystallization of the phases (*9*). According to chemical thermodynamics, the distribution of two components A and B in coexisting binary solid solutions α and β, which equilibrated at a certain pressure and temper-

ature, is given by a smooth curve when the ratio of the components (A/B) in α is plotted against a similar ratio (A/B) in β. An ion-exchange reaction which depends only on pressure and temperature and the compositions of the phases may be expressed as

$$A\text{-}\alpha + B\text{-}\beta \rightleftharpoons A\text{-}\beta + B\text{-}\alpha \qquad (1)$$

If both α and β are ideal solutions, the distribution points (A/B) in α versus (A/B) in β must fall on a straight line whose slope is a function of pressure and temperature. For nonideal binary solutions, the distribution points define a smooth curve if equilibrium is established. A scatter of distribution points for metamorphic rocks indicates disequilibrium. For a multicomponent solution, however, scatter may result from nonideal ionic substitutions in the phases under consideration as demonstrated by Kretz (*8*).

Data on the chemical composition of minerals in the charnockites have been presented by several investigators (*4, 10, 11*). Orthopyroxene ($FeSiO_3$-$MgSiO_3$) and clinopyroxene ($FeCaSi_2O_6$-$MgCaSi_2O_6$) are two quasi-binary solutions commonly present in these rocks. First, I will examine the evidence of chemical equilibrium in the distribution of Fe^{2+} and Mg^{2+} and other ions in coexisting minerals, particularly in the two pyroxenes. I have assumed that the charnockites have formed in a narrow range of pressure and temperature, irrespective of their geographic occurrence.

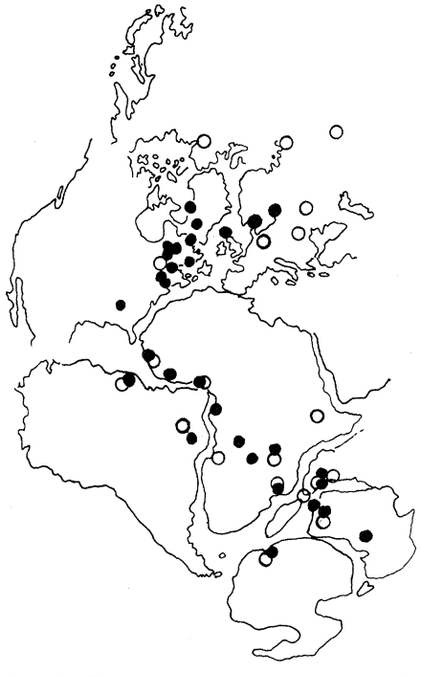

Fig. 1. Charnockite occurrences (open circles) shown on Hurley and Rand's (*2*) map of the granulite facies rocks (closed circles). Since data on charnockite ages are meager and have not been critically evaluated, no relationship in age or time can yet be implied.

Table 1. A summary of estimates of the temperature of crystallization of charnockite pyroxenes.

Area	Temperature (°C)
India	825 to 905
Adirondacks, New York	800 to 900
Uganda	850
Sweden	800 to 870
Finland	835 to 915
Norway	800
Sudan	800
Poland	800 to 900

Figure 2 shows the Mg/Fe ratio for clinopyroxene plotted against the same ratio for orthopyroxene in charnockites from India, Scandinavia, and New York (*4, 10, 11*). The Mg/Fe ratios of coexisting pyroxenes in rocks of the Stillwater igneous complex (*12*) have also been plotted for comparison. There is a distinct difference in the way the data from the two groups of rocks plot. The data can be closely fitted by two straight lines with average distribution coefficients, K_D (K_D = Mg/Fe in orthopyroxene divided by Mg/Fe in clinopyroxene), of 0.6 for the charnockites and 0.75 for the Stillwater rocks. Kretz [see (*9*)] found similarly that the K_D values for metamorphic rocks lie close to 0.54 and those for igneous rocks close to 0.73. Saxena has discussed the effects of pressure and temperature on K_D (*9*). For the Stillwater rocks, McCallum (*12*) has inferred a temperature range of crystallization of 1000° to 1200°C. The charnockite pyroxenes contain a higher Ca content than the Stillwater pyroxenes, but the low Ca content in igneous pyroxenes has been clearly recognized to be due to the high temperature of crystallization (*13*). For Fe-free pyroxenes, the Ca content is a measure of the temperature of crystallization (*13*). Figure 3 shows the distribution of Cr in coexisting pyroxenes in Adirondack rocks (*14*) and in Stillwater rocks (*12*), and Fig. 4 shows the Mn distribution in several coexisting minerals in Varberg charnockites (*11*). The orderly distribution of ions in Figs. 2 through 4 indicates that pyroxenes in charnockites crystallized in chemical equilibrium over a narrow range of pressure and temperature and that the temperature of formation of charnockites was distinctly different from those of igneous plutons. The charnockite temperature of formation lies in the subsolidus range for most basic and intermediate bulk chemical compositions.

In an effort to estimate the pressure and temperature of formation of charnockites, I will use two independent lines of approach. The first consists of the use of an empirically derived, two-pyroxene geothermometer, and the second method is based on experimentally determined phase equilibrium relations.

The compositions of coexisting pyroxenes in Fe-poor systems have been used extensively in the literature (*13*) to estimate the temperature of pyroxene crystallization. The problems of pyroxene geothermometry in ultramafic rocks (*13*) are different from those in charnockites. The charnockite pyroxenes are poor in Al [usually less than 2.0 percent (by weight) of Al_2O_3] and relatively rich in Fe. A thermodynamic model of a two-pyroxene geothermometer based on the compositional data on coexisting pyroxenes of Ross and Huebner (*15*) has been proposed by Saxena (*16*). This thermometer does not take into account the effect of pressure and of such components as Al^{3+}, Fe^{3+}, and Ti^{4+} in pyroxenes. Using this thermometer, Gross (*17*) determined the temperatures of crystallization of over 50 coexisting pyroxenes in charnockites (Table 1). The estimated temperatures appear to lie in the range 800° to 925°C with an average value of 870°C. At present, experimental data on the compositions of coexisting pyroxenes are inadequate and the activity-composition relations are incompletely

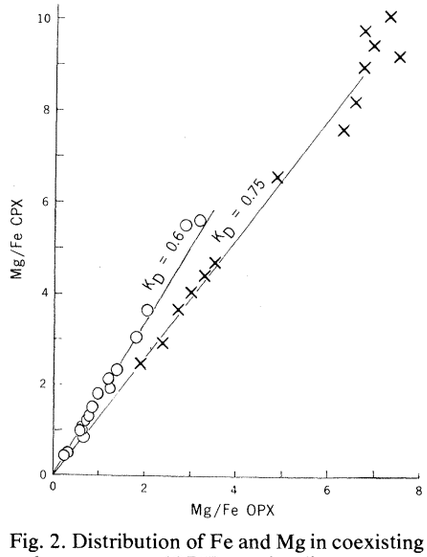

Fig. 2. Distribution of Fe and Mg in coexisting orthopyroxene (*OPX*) and clinopyroxene (*CPX*). Open circles represent charnockites from India, Sweden, Norway, Finland, and New York. Each circle represents more than one sample. Data on igneous pyroxenes from the Stillwater complex have also been plotted (crosses) for comparison.

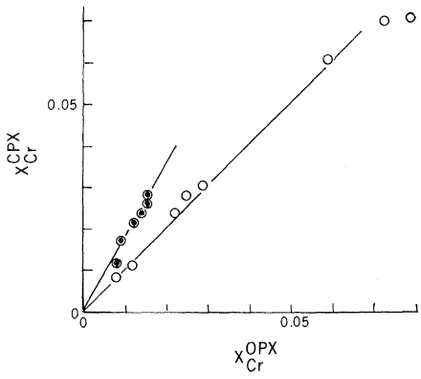

Fig. 3. Distribution of Cr in coexisting orthopyroxens (*OPX*) and clinopyroxene (*CPX*): X = Cr/(Cr + Al). Open circles represent Stillwater samples, and closed circles represent the Adirondack granulites.

known. Therefore, it is not possible to estimate errors in the temperature determination; however, the range of 800° to 900°C for the formation of charnockites appears reasonable on the basis of petrogenetic considerations as discussed below.

Figure 5 shows a collection of some experimentally determined pressure-temperature phase equilibria relevant to the establishment of the pressure and temperature of formation of charnockites. Curve 1 represents the critical mixing of albite ($NaAlSi_3O_8$) and orthoclase ($KAlSi_3O_8$) as determined by Morse (*18*). At temperatures below curve 1 an alkali feldspar solid solution unmixes and forms perthite and antiperthite textures which are common in charnockites. The alkali feldspars in charnockites, however, contain Ca in addition. The critical curve shifts toward higher temperatures as a function of increasing Ca content (*18*). The occurrence of perthite in charnockites, therefore, indicates a minimum temperature of crystallization of 700°C.

Curve 2 represents the reaction of tremolite [$Ca_2Mg_5Si_8O_{22}(OH)_2$] with diopside ($CaMgSi_2O_6$), enstatite ($MgSiO_3$), quartz (SiO_2), and water (*19*):

$$Ca_2Mg_5Si_8O_{22}(OH)_2 \rightleftharpoons 2\ CaMgSi_2O_6 + 3\ MgSiO_3 + SiO_2 + H_2O \quad (2)$$

In charnockites two pyroxenes and the aluminous amphibole hornblende are commonly present. Hornblende differs from tremolite in containing Al and some Na. All three minerals contain significant concentrations of the Fe end-members. A theoretical analysis of the equilibrium in Eq. 2 indicates that, although the effect of increasing Fe in the minerals shifts the equilibrium curve to lower temperatures (*20*), the effect of introducing Al in amphibole would be the opposite.

According to Luth's (*21*) work, an assemblage in the Fe-free system containing phlogopite [$KMg_3AlSi_3O_{10}(OH)_2$], alkali feldspar ($KAlSi_3O_8$), enstatite, and quartz is stable in the field between curves 3 and 4 representing the reactions:

$$KMg_3AlSi_3O_{10}(OH)_2 + 3\ SiO_2 \rightleftharpoons KAlSi_3O_8 + 3\ MgSiO_3 + H_2O \quad (3)$$

$$KAlSi_3O_8 + MgSiO_3 + SiO_2 + H_2O \rightleftharpoons \text{liquid melt} \quad (4)$$

Thermodynamic considerations indicate that, because Fe and Mg are distributed approximately equally between biotite and orthopyroxene (*11*), the presence of Fe in the charnockite assemblage would not change the equilibrium relations significantly.

Equilibrium pressure and temperatures for Eqs. 2 through 4 (Fig. 5) have been determined under the condition that the H_2O vapor pressure is equal to the total pressure acting on the solids. In the metamorphism of granulite facies, the H_2O vapor pressure may be lower than the total pressure. The equilibrium temperature for Eqs. 2 through 4 would be higher under such conditions.

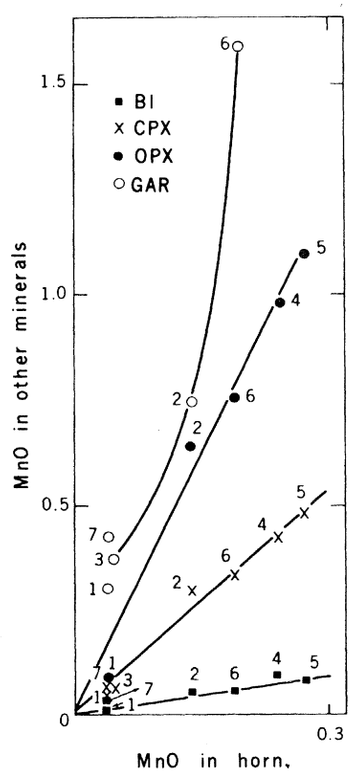

Fig. 4. Distribution of MnO in coexisting minerals in charnockites from Varberg, Sweden: *BI*, biotite; *CPX*, clinopyroxene; *OPX*, orthopyroxene; and *GAR*, garnet. The orderly distribution in all the phases implies a close approach to equilibrium during metamorphism.

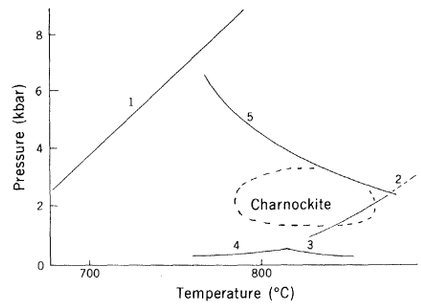

Fig. 5. Phase diagram showing the possible pressure-temperature field for the formation of charnockites. The curves represent the following equilibria: curve 1, critical mixing of albite and orthoclase; curve 2, tremolite ⇌ diopside + enstatite + quartz + H_2O vapor; curve 3, phlogopite + quartz ⇌ orthoclase + enstatite + H_2O vapor; curve 4, orthoclase + quartz + enstatite + H_2O vapor ⇌ liquid; and curve 5, anorthite + quartz + H_2O vapor ⇌ liquid.

The temperature of formation of charnockites as estimated from pyroxene geothermometry is clearly in conformity with the experimental results on the stability of the mineral assemblages commonly found in these rocks. The pressure of formation of the charnockites cannot be very much greater than that of the reaction of anorthite ($CaAl_2Si_2O_8$), quartz, and water in Eq. 5:

$$CaAl_2Si_2O_8 + SiO_2 + H_2O \rightleftharpoons \text{liquid melt} \quad (5)$$

If the H_2O vapor pressure is less than the pressure on the solids, the equilibrium temperature and pressure would increase. However, since hydrous phases such as hornblende and biotite are present in many charnockites, the H_2O vapor pressure cannot be too low. The equilibrium temperature and pressure in Eq. 5 are also functions of the concentrations of Na and Ca in plagioclase. Increasing Na, for example, would shift the equilibrium curve to lower pressures. Since plagioclase in charnockites is commonly intermediate in composition between anorthite and albite ($NaAlSi_3O_8$), the pressure-temperature field for the formation of charnockites may be delineated as shown in Fig. 5.

The time-and-space relationship of charnockites in different parts of the world is unclear. The few ages of charnockites that are available show a range of 1000×10^6 to 3500×10^6 years. For example, Polish charnockites are 1250×10^6 to 1350×10^6 years old (*22*), whereas Minnesota charnockites are 3500×10^6 years old (*23*). In at least four different parts of the world, the char-

nockites or the associated high-grade metamorphic rocks of granulite facies show a close correspondence in age ($\times 10^6$ years) (*14, 24*): Adirondacks region of New York, 1120; eastern India, 1300 to 1520; Podlasie, Poland, 1250 to 1350; and Sweden and Norway, 900 to 1300.

According to the compilation of Engel *et al.* (*25*), the ages of the rocks of the granulite facies show a significant modal class around $1200:10^6$ years ago. It seems that during this period in the earth's history charnockites must also have recrystallized, and temperatures in the range of 800° to 900°C were attained at shallow depths of 6 to 12 km. Such geothermal gradients of the order of 70° to 100°C per kilometer would also lead to the melting of the mantle rocks. The significance of the information on the pressure and temperature of formation of charnockites presented above cannot be fully realized unless age data on charnockites are collected for the different regions of the world. The age relationships could show whether the formation of charnockites was due to a global thermal event such as that proposed by Herz (*26*) for anorthosite formation or whether they formed in isolated events unrelated in space and time.

S. K. SAXENA

Department of Geology, Brooklyn College, City University of New York, Brooklyn 11210

References and Notes

1. R. A. Howie, *Sci. Progr. (London)* **52**, 628 (1964).
2. P. M. Hurley and J. R. Rand, *Science* **164**, 1229 (1969).
3. C. Muthuswami, *Proc. Indian Acad. Sci.* **37**, 730 (1956).
4. R. A. Howie, *Trans. R. Soc. Edinburgh* **62**, 725 (1955).
5. F. H. Hubbard, *Geol. Foeren. Stockholm Foerh.* **97**, 223 (1976).
6. "Charnockitization" refers to reactions leading to the metamorphism of igneous or sedimentary rocks to charnockites.
7. These charnockites were emplaced during the time of granulite facies metamorphism and must have recrystallized as indicated by pyroxene geothermometry (see text).
8. R. Kretz, *J. Geol.* **67**, 371 (1959).
9. S. K. Saxena, *Thermodynamics of Rock-Forming Crystalline Solutions* (Springer-Verlag, New York, 1973), p. 180.
10. C. Leelanandam, *Mineral. Mag.* **36**, 153 (1967); S. K. Saxena, *Contrib. Mineral. Petrol.* **20**, 177 (1969); ——— and N. B. Hollander, *Neues Jahrb. Mineral. Monatsh.* **2**, 85 (1969); S. K. Saxena, unpublished data.
11. S. K. Saxena, *Am. Mineral.* **53**, 1674 (1968).
12. I. S. McCallum, thesis, University of Chicago (1968).
13. F. R. Boyd, *Geochim. Cosmochim. Acta* **37**, 2533 (1973); J. Mercier and N. Carter, *J. Geophys. Res.* **80**, 3349 (1975).
14. A. E. J. Engel, C. G. Engel, R. G. Havens, *J. Geol.* **72**, 131 (1964).
15. M. Ross and J. S. Huebner, paper presented at the International Symposium on Geothermometry and Geobarometry, Pennsylvania State University, October 1976.
16. S. K. Saxena, *Am. Mineral.* **61**, 643 (1976).
17. J. Gross, in preparation.
18. S. A. Morse, *J. Petrol.* **11**, 221 (1970); *Carnegie Inst. Washington Yearb.* **67**, 120 (1968).
19. F. R. Boyd, in *Researches in Geochemistry*, P. H. Abelson, Ed. (Wiley, New York, 1959), pp. 377–397.
20. R. F. Mueller and S. K. Saxena, *Chemical Petrology* (Springer-Verlag, New York, 1977), p. 177.
21. W. C. Luth, *J. Petrol.* **8**, 372 (1967).
22. W. Ryka, *Int. Geol. 23rd Congr. Abstr.* (1968).
23. V. Rama Murthy, personal communication.
24. V. Aswathanarayana, *Can. J. Earth Sci.* **5**, 59 (1968); E. Welin, *Geol. Foeren. Stockholm Foerh.* **88**, 29 (1966); P. Pasteels and J. Michot, *Nor. Geol. Tidsskr.* **55**, 111 (1975).
25. A. E. Engel, S. P. Itson, C. G. Engel, D. M. Stickney, E. J. Cray, Jr., *Geol. Soc. Am. Bull.* **85**, 843 (1974).
26. N. Herz, *Science* **164**, 944 (1969).

14 April 1977; revised 9 June 1977

Pituitary Nuclear 3,5,3′-Triiodothyronine and Thyrotropin Secretion: An Explanation for the Effect of Thyroxine

Abstract. *An excellent correlation was observed between nuclear triiodothyronine (T_3) and the ensuing suppression of thyrotropin (TSH) after a single intravenous injection of T_3 to thyroidectomized (hypothyroid) rats. At 1 and 2 hours after injection of thyroxine (T_4), in amounts equally potent to the administered T_3 in terms of acute suppression of TSH, the same quantities of T_3 were found in the pituitary nuclei. Virtually no nuclear T_4 was present, and plasma T_3 was negligible at these short intervals after T_4 injection. These results suggest that suppression of TSH release in hypothyroid rats occurs by interaction of T_3 with the nuclear receptor of the thyrotroph. After T_4 injection, the T_3 found in the nucleus is derived from rapid intrapituitary monodeiodination.*

There is strong evidence supporting the cell nucleus as the site of initiation of thyroid hormone action (*1*). The degree of occupancy of nuclear binding sites by triiodothyronine (T_3) has been correlated with the quantity of malic enzyme and mitochondrial α-glycerophosphate dehydrogenase in hepatic tissue (*1, 2*) and with growth hormone synthesis and inhibition of prolactin secretion in GH_1 pituitary cells in culture (*3*). Physiological studies have indicated that in the liver, thyroxine (T_4) produces its thyromimetic effect primarily by serving as a source of T_3. Inhibition of the conversion of T_4 to T_3 by 6-*n*-propyl-2-thiouracil (PTU) blocks a significant fraction of the hepatic effect of T_4 (*4*).

Recently, Larsen and Frumess (*5*) reported comparative studies on the effects of T_3 and T_4 in thyroidectomized rats. In these experiments, T_4 (800 ng per 100 g body weight) caused the same degree of acute inhibition of thyrotropin (TSH) release as rapidly as did T_3 at 70 ng per 100 g. Interestingly, the serum T_3 concentrations in animals injected with T_4 increased only minimally into the low to normal range, contrasting with the sharp elevation in the animals injected with T_3. In the same experiments, PTU pretreatment did not block the TSH-suppressive effect of T_4. From previous studies with hepatic nuclear T_3 receptors and those from GH_1 pituitary cells in culture, it would be assumed that T_4 binds to the T_3 pituitary nuclear receptor with at most one-tenth the affinity of T_3 (*1, 6*). Nevertheless, our data, as well as those of other investigators, could be interpreted as showing that T_4 has a direct inhibitory effect on TSH release (*7*). Alternatively, in light of previous studies demonstrating tracer T_3 in the anterior pituitary after injection of tracer T_4 (*8*), we considered the possibility that T_4 may be rapidly monodeiodinated to T_3 in the thyrotroph, providing T_3 directly to the nuclear receptor. The evidence presented in this report indicates that this, in fact, occurs, and that suppression of plasma TSH after either T_3 or T_4 injection is correlated both temporally and quantitatively with the occupancy of the pituitary nuclear receptor sites by T_3.

To establish a correlation between pituitary nuclear T_3 receptor occupancy and serum TSH, we used the protocol previously described (*5*). Thyroidectomized male Sprague-Dawley rats were allowed several months to become hypothyroid. Either T_3 (70 ng per 100 g) or T_4 (800 ng per 100 g) or both were injected intravenously with [^{125}I]T_3 (specific activity, ~ 500 μc/μg) or [^{125}I]T_4 (specific activity, ~ 6000 μc/μg)—15 and 150 μc per 100 g, respectively. [^{131}I]Albumin was injected simultaneously with [^{125}I]T_4 to allow corrections for the plasma contribution to tissue radioactivity [(*6*); see also (*12*) below]. All animals received 2 mg of NaI intraperitoneally to dilute the $^{125}I^-$ pool. Animals were killed at indicated times by aortic exsanguination. Rats injected with T_4 were then perfused with 20 to 25 ml of cold 0.15*M* NaCl to minimize trapped plasma in the tissues. Anterior pituitaries were removed and weighed, and nuclei were prepared essentially as described elsewhere (*9*). Recovery of pituitary DNA was 6.5 to 7.5 mg/g. The nuclei were intact and uncon-